

1 *bioRxiv*

2

3

4

5

6

7

8

9

10

11

12 **Mis-perception of motion in depth originates from an** 13 **incomplete transformation of retinal signals**

14

15 T. Scott Murdison^{1,2,3}, Guillaume Leclercq⁴, Philippe Lefèvre⁴ and Gunnar
16 Blohm^{1,2,3}

17

18 ¹Centre for Neuroscience Studies, Queen's University, Kingston, Ontario,
19 Canada

20

21 Canadian Action and Perception Network (CAPnet), Toronto, Ontario, Canada

22

23 ³Association for Canadian Neuroinformatics and Computational Neuroscience
24 (CNCN), Kingston, Ontario, Canada

25

26 ⁴ICTEAM and Institute for Neuroscience (IoNS), Université catholique de
27 Louvain, Louvain-La-Neuve, Belgium

28

29 28 total pages

30

31 5 figures, 0 supplementary figures

32

33 0 tables

34

35 221 words in Abstract

36

37 **Contact:**

38

39 Scott Murdison

40

41 Centre for Neuroscience Studies (CNS), Queen's University

42

43 Botterell Hall

44

45 Kingston, Ontario, Canada K7L3N6

46

47 Email: scott.murdison@oculus.com

39 **Abstract**

40 Depth perception requires the use of an internal model of the eye-head geometry
41 to infer distance from binocular retinal images and extraretinal 3D eye-head
42 information, particularly ocular vergence. Similarly for motion in depth perception,
43 gaze angle is required to correctly interpret the spatial direction of motion from
44 retinal images; however, it is unknown whether the brain can make adequate use
45 of extraretinal version and vergence information to correctly interpret binocular
46 retinal motion for spatial motion in depth perception. Here, we tested this by
47 asking participants to reproduce the perceived spatial trajectory of an isolated
48 point stimulus moving on different horizontal-depth paths either peri-foveally or
49 peripherally while participants' gaze was oriented at different vergence and
50 version angles. We found large systematic errors in the perceived motion
51 trajectory that reflected an intermediate reference frame between a purely retinal
52 interpretation of binocular retinal motion (ignoring vergence and version) and the
53 spatially correct motion. A simple geometric model could capture the behavior
54 well, revealing that participants tended to underestimate their version by as much
55 as 17%, overestimate their vergence by as much as 22%, and underestimate the
56 overall change in retinal disparity by as much as 64%. Since such large
57 perceptual errors are not observed in everyday viewing, we suggest that other
58 monocular and/or contextual cues are required for accurate real-world motion in
59 depth perception.

60

61 *Keywords: ocular vergence, horizontal version, depth perception, motion*

62 *perception, reference frames*

63 **Introduction**

64 Stereoscopic vision is crucial for perceiving and acting on objects moving around
65 us in three-dimensional (3D) space. Consider a batter in baseball: to accurately
66 swing at an approaching pitch, the visuomotor system must first estimate the 3D
67 spatial motion of the ball in space from two 2D retinal projections (Batista, Buneo,
68 Snyder, & Andersen, 1999; Blohm & Crawford, 2007; Blohm, Khan, Ren,
69 Schreiber, & Crawford, 2008; Chang, Papadimitriou, & Snyder, 2009). That
70 means the brain has the difficult task of assigning coordinating points on each
71 retina to the moving object and using an internal model of the eye-head geometry
72 to accurately compute its 3D egocentric distance (Blohm et al., 2008). However,
73 exactly which signals are used to extract motion-in-depth from binocular images
74 is unclear.

75

76 Part of the confusion comes from an overabundance of available depth cues.
77 Motion-in-depth cues can arise from both retinal and extraretinal sources and can
78 be monocular or binocular. Monocular cues include retinal image features (e.g.,
79 shading, texture, defocus blur, perspective, optical expansion, kinetic depth cues,
80 motion parallax, etc.) (Guan & Banks, 2016; Held, Cooper, & Banks, 2012;
81 Zannoli, Love, Narain, & Banks, 2016; Zannoli & Mamassian, 2011), and ocular
82 accommodation (Guan & Banks, 2016; Mon-Williams & Tresilian, 2000).
83 Binocular cues include retinal disparity, inter-ocular velocity differences, ocular
84 vergence (Mark Mon-Williams & Tresilian, 1999; Mon-Williams, Tresilian, &
85 Roberts, 2000) and version angles (Backus, Banks, Van Ee, & Crowell, 1999;

86 Banks & Backus, 1998). Ultimately, however, because retinal disparity varies
87 non-uniformly with 3D eye-in-head orientation (Blohm et al., 2008), retinal signals
88 alone are insufficient to estimate motion-in-depth; rather, the visual system must
89 account for the full 3D geometry of the eye and head (Blohm et al., 2008).
90 Indeed, Blohm et al. (2008) demonstrated that the visual system accounts for 3D
91 eye-in-head orientation to accurately reach to static objects in depth, but how this
92 finding extends to *moving* objects in depth is unclear. Here, we attempt to answer
93 this question by asking participants to reconstruct motion-in-depth trajectories
94 from only binocular depth cues across various horizontal vergence and version
95 angles.

96

97 Another open question is how motion-in-depth perception depends on retinal
98 eccentricity. Although the magnitude of binocular disparity increases with retinal
99 eccentricity (Blohm et al., 2008), many of the observed disparity-selective cortical
100 cells are tuned for small-magnitude disparities (DeAngelis & Uka, 2003), hinting
101 that binocular signals may play a large role for depth perception near the fovea
102 but not in the periphery. Convincing work from Held et al. (2012) found that
103 position-in-depth is extracted in a complementary way: using mostly binocular
104 disparity signals at the fovea and using mostly defocus blur in the periphery.
105 Whether motion-in-depth estimates are similarly eccentricity-dependent,
106 however, is unclear.

107

108 In this study, we asked participants to reproduce the perceived horizontal depth
109 spatial trajectory of an isolated point stimulus observed either foveally or
110 peripherally under different vergence and version angles. We found large
111 systematic errors in the perceived motion trajectory that seemed to reflect an
112 intermediate reference frame between purely retinal and spatial coordinates. A
113 simple geometric model could capture the behavior well, revealing that
114 participants tended to underestimate their version, overestimate their vergence,
115 and underestimate the overall change in retinal disparity. These findings suggest
116 that real-world motion-in-depth estimation is an eccentricity-dependent process
117 that relies heavily on the use of monocular and/or contextual cues.

118

119 **Materials and methods**

120 *Participants*

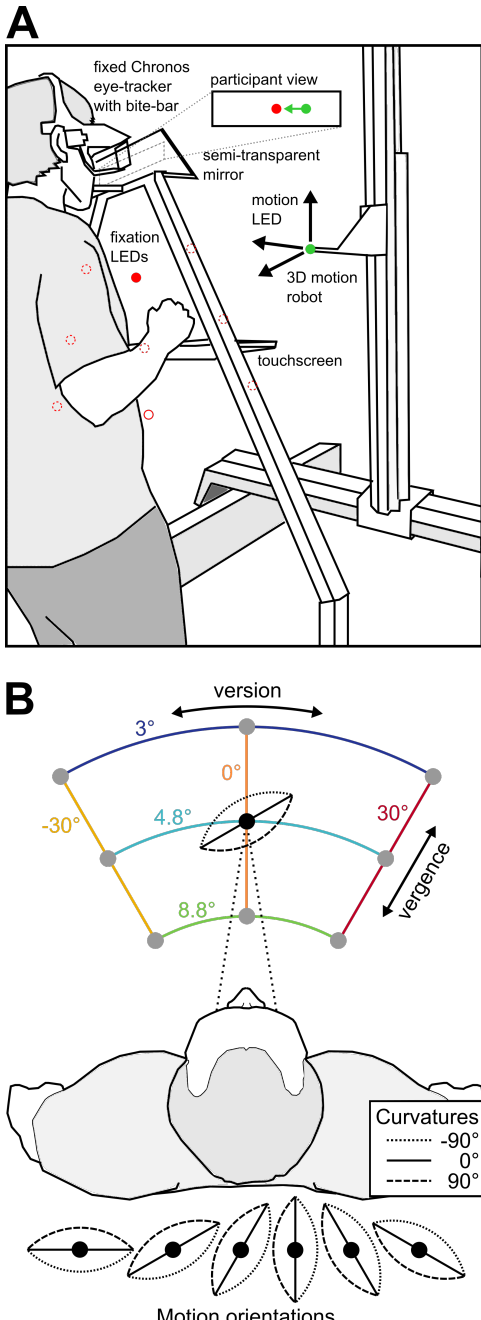
121 In total, 12 participants (age 22-35 years, 9 male) were recruited for two
122 experiments after informed consent was obtained. 11 of 12 participants were
123 right-handed and all participants were naïve as to the purpose of the experiment.
124 All participants had normal or corrected-to-normal vision and did not have any
125 known neurological, oculomotor, or visual disorders. We also evaluated
126 participants' stereoscopic vision using the following tests: Bagolini striated
127 glasses test (passed by all participants), Worth's four dot test (passed by all
128 participants), and TNO stereo test (all but 2 participants could detect disparities
129 ≤ 60 seconds of arc). All procedures were approved by the Queen's University
130 Ethics Committee in compliance with the Declaration of Helsinki.

131

132 *Experimental paradigm*

133 We used a novel 3D motion paradigm to determine how motion-in-depth is
134 perceived across different horizontal version and vergence angles in complete
135 darkness. This paradigm is illustrated in Fig. 1. In panel A, we show the physical
136 setup with the array of red light-emitting diodes (LEDs) representing possible
137 fixation targets (FTs; filled red circle represents the sample trial's illuminated FT)
138 and the green LED (filled green circle) representing the motion target (MT), which
139 was attached to the arm of a custom 3D gantry system (Sidac Automated
140 Systems, North York, ON) that was positioned at the same elevation as the eyes
141 and moved within the horizontal depth (x-y) plane. At the end of target motion,
142 participants were instructed to reconstruct the motion of this target using a stylus
143 on the touchscreen in front of them. On each trial, the FT was reflected through a
144 mirror oriented at 45° and positioned at the level of the eyes, such that the
145 participant perceived the FT as located in the same horizontal depth plane as the
146 MT. Other key elements in the physical setup included a stationary Chronos C-
147 ETD 3D video-based eye tracker (Chronos Vision, Berlin, Germany) with an
148 attached bite-bar for head stabilization to ensure stable fixation on the FT during
149 target motion. This physical arrangement allowed us to present FTs in the MT
150 plane while avoiding physical collisions (panel B) with FTs positioned at nine
151 different locations (corresponding to three horizontal version angles, -30°, 0° and
152 30°, and three vergence angles, 3°, 4.8° and 8.8°) and 18 different motion

153 trajectories (six orientations spaced equally from 0° to 180°, with three possible
154 curvatures) purely in the horizontal depth plane.



155

156 **Figure 1: Apparatus and virtual setup.** A Experimental apparatus, including
157 3D motion robot with attached MT LED (green), frontoparallel arc-array of 9 FT
158 LEDs (red), 45° oriented semi-transparent mirror, fixed Chronos eye tracker, and
159 touchscreen. For a given trial, one of the FT LEDs is illuminated and reflected at
160 eye-level using the semitransparent mirror. Meanwhile, the motion robot moves
161 the MT LED in the horizontal depth plane also at eye level, creating the

162 participant view shown in the inset. **B** Virtual setup created by the experimental
163 apparatus and tested motion trajectories, with 6 orientations (30° steps from 0° to
164 150°) and 3 curvatures (-90°, 0° and 90°).

165

166 *Procedure*

167 Participants knelt, supported by the custom apparatus, in complete darkness.

168 Each trial was defined by three phases: (1) fixation, (2) motion observation and

169 (3) reporting. During the fixation phase (0 ms –1500 ms), participants fixated a

170 randomly selected, illuminated FT from the array of nine LEDs. During the motion

171 observation phase (1500 ms –3200 ms), participants maintained fixation on the

172 FT while the MT was displaced by the robot. That MT displacement either

173 occurred in the immediate space around the FT (foveal condition) or around the

174 central (non-illuminated) LED while the participant maintained fixation on the FT

175 (peripheral condition). Participants were asked to memorize its trajectory in the x-

176 y plane. During the reporting phase (3200 ms – trial end), participants were

177 asked to remove their head from the bite-bar and trace the perceived spatial

178 trajectory using a stylus on a touchscreen, illuminated using a single bright LED

179 for this trial phase only. The light remained on until a response was recorded,

180 and participants were free to restart their trace at any time. They touched the

181 lower right corner of the screen in order to end the current trial, triggering the

182 start of the next trial.

183

184 *Trial selection*

185 We recorded a total of (9 fixation targets * 3 curvatures * 6 orientations * 2 motion

186 location conditions =) 324 trials for each participant (324 trials * 13 participants =

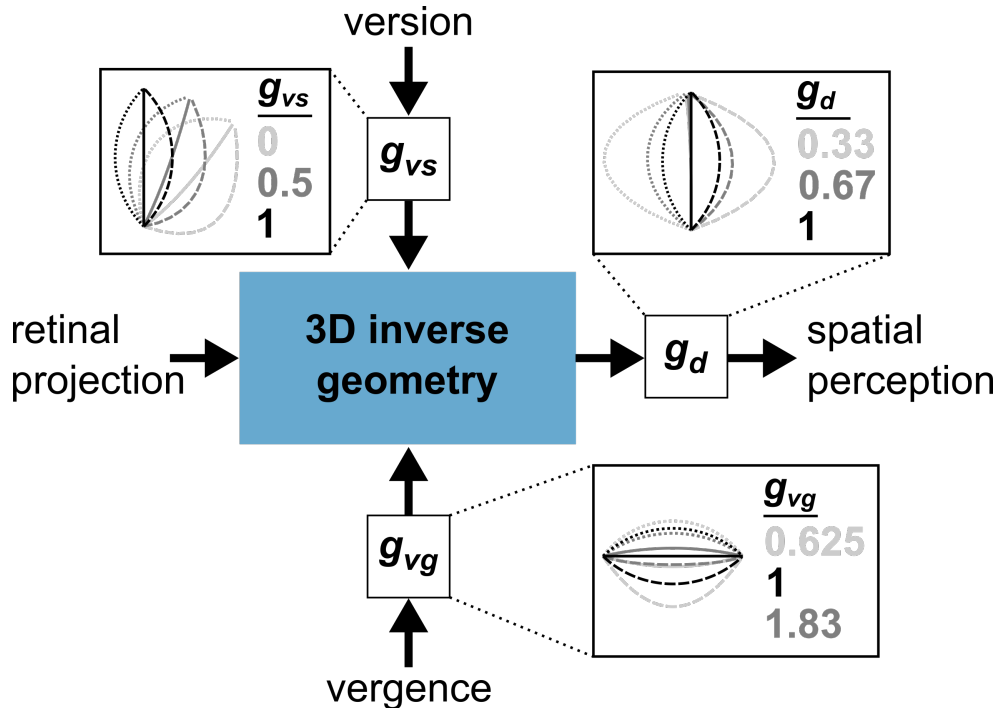
187 4212 total trials). Each trial type was randomly interleaved throughout 10 blocks
188 (per participant) but the order was the same across all participants. This allowed
189 us to pool the responses together across conditions and participants for graphical
190 purposes, as there were no within-participant trial repetitions (model fits were
191 performed on individual trajectories). Upon offline analysis, we discovered that
192 one participant consistently failed to perform the reconstruction portion of the
193 task as instructed: the participant drew the motion backwards and we therefore
194 excluded his data from the analysis, leaving 12 participants (3888 total trials). Of
195 these trials, we examined recorded eye movement data and removed trials
196 containing eye movements or blinks during the motion phase of each trial,
197 leaving 3869 valid trials for analysis.

198

199 *3D binocular kinematic model*

200 We developed a 3D model of the binocular retina-eye-head geometry to predict
201 how behavioral motion reconstructions might vary across version and vergence
202 angles (Blohm et al., 2008). This model consisted of three primary stages: retinal
203 motion encoding, inverse modeling and spatial motion decoding. First, we
204 computed the binocular retinal projections of the motion stimulus, given the
205 current eye and head orientations (retinal motion encoding stage). Second, we
206 moved the eyes together to the inverse estimates of version and vergence
207 angles during the encoding of retinal motion (inverse modeling stage). We then
208 back-projected the retinal coordinates into space and computed the 3D location
209 of the rays' intersection, representing the decoded depth (spatial decoding

210 stage). Although in reality we computed all three stages of this model to obtain
211 our trajectory estimates, we simplify the graphical representation of this model in
212 Figure 2: focusing on the inverse modeling stage, where we varied the
213 contributions of extraretinal signals.



214
215 **Figure 2: Inverse modeling stage of the 3D binocular kinematic model to**
216 **generate retinal and partial model predictions.** Insets show individual
217 parameter effects on reconstructed traces. The effects of version gain are shown
218 for a fixation version angle of 30deg; the effects of vergence gain are shown for a
219 fixation vergence of 4.8deg; the effects of depth gain are shown for trajectories
220 with an orientation of 90deg.
221

222 This modeling framework allowed us to describe the reconstructed trajectories by
223 varying the contributions of version (version gain, g_{vs}) and vergence (vergence
224 gain, g_{vg}) to the inverse model, and motion purely in depth (depth gain, g_d). Each
225 parameter accounted for a different aspect of the trajectory (shown in Figure 2
226 insets). To produce the retinal prediction, we set the version gain to 0 and used a
227 constant vergence gain of 1. Importantly, this retinal prediction arbitrarily

228 assumes that vergence is 100% accounted for. Note that, because our model
229 computes the spatial intersection of the binocular back-projections, vergence
230 gains had to be greater than 0 (otherwise the back-projections would be parallel).

231

232 For each participant, we initialized the parameters for the reconstructed
233 trajectories using a brute-force, 8000 point least-squares method over the full
234 plausible range of parameters (20 linearly spaced values for each parameter).
235 This was followed by a 512 point least-squares fine fitting method within a +/-
236 10% range for g_{vs} , g_{vg} and g_d around the initialized parameters (8 linearly spaced
237 values for each parameter). We performed this exact optimization procedure
238 separately for each vergence angle to avoid confounding vergence effects. In
239 total, we computed the fits of $(3*(8000+512) =) 25,536$ total parameter
240 combinations. This optimization provided parameter estimates that consistently
241 accounted for behavioral variability, with each participant's R-squared values
242 >0.93 in both motion conditions.

243

244 *Statistical analyses*

245 Group-level statistical tests primarily consisted of two-tailed Student t-tests. We
246 also performed paired t-tests when appropriate for comparing parameters across
247 conditions. The rest of the statistical treatment of the data consisted primarily of
248 computing correlation coefficients and regression analyses.

249

250 **Results**

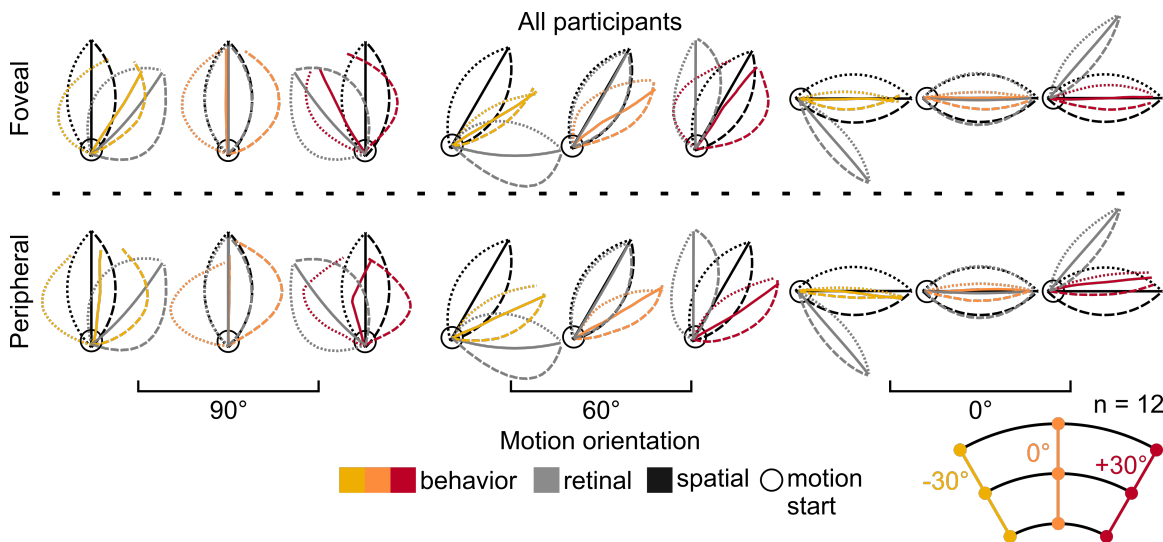
251 We sought to determine how visual perception accounts for binocular eye
252 orientation when reconstructing motion in depth. To do this, we designed a novel
253 paradigm in which participants reconstructed motion of an LED in the horizontal
254 depth plane presented either foveally or peripherally on the retina, while fixated in
255 one of nine randomly selected version and vergence orientations. After observing
256 the motion, participants generated this reconstruction using a touchscreen
257 positioned in the coronal plane directly in front of them. We then analyzed these
258 reconstructed trajectories to determine how they varied across eye orientation
259 and motion condition. To generate model predictions for the reconstructed
260 signals across changes in version and vergence angles, we developed a 3D
261 model of the binocular eye-head geometry (Figure 2, see *Methods* for model
262 details). This model allowed us to characterize the eye orientation signals
263 accounted for by the perceptual system.

264
265 Reconstructed trajectories deviated from both the spatial (physical) and retinal
266 (see *Methods*) predictions for both foveal and peripheral motion across all
267 vergence angles. These trajectories are shown alongside their predictions for
268 three representative motion orientations in Figure 3, averaged across all
269 participants and vergence angles for foveal (top row) and peripheral motion
270 (bottom row). These comparisons revealed both an angular displacement
271 between the trajectories during nonzero version as well as a compression of the
272 behavioral traces in the depth dimension across motion orientations; however,

273 these patterns were not consistent for both motion conditions, as only the
274 compression effect was obvious in the peripheral case.

275

276



277

278 **Figure 3: Average across-participant foveal and peripheral reconstructed**
279 **motion**, compared with spatial and retinal predictions. Note that reconstructed
280 traces were normalized in amplitude to the spatial and retinal predictions.

281

282 The reconstructed trajectories matched neither the spatial nor retinal hypotheses,
283 suggesting that the perceptual system only partially transformed the retinal MT
284 trajectories into spatial coordinates. To capture the extent to which the perceptual
285 system encoded binocular eye orientations and estimated motion purely in the
286 depth dimension (i.e. when the MT was stationary on the retina), we used a two-
287 step least-squares algorithm to optimize the g_{vs} , g_{vg} and g_d inverse model
288 parameters for the behavioral trajectories (see *Methods* for detailed explanation
289 of optimization algorithm). The results of this optimization are shown in Figure 4
290 at both the single participant level (panel A) and group level (panel B) for both the
291 foveal and peripheral motion conditions.

292

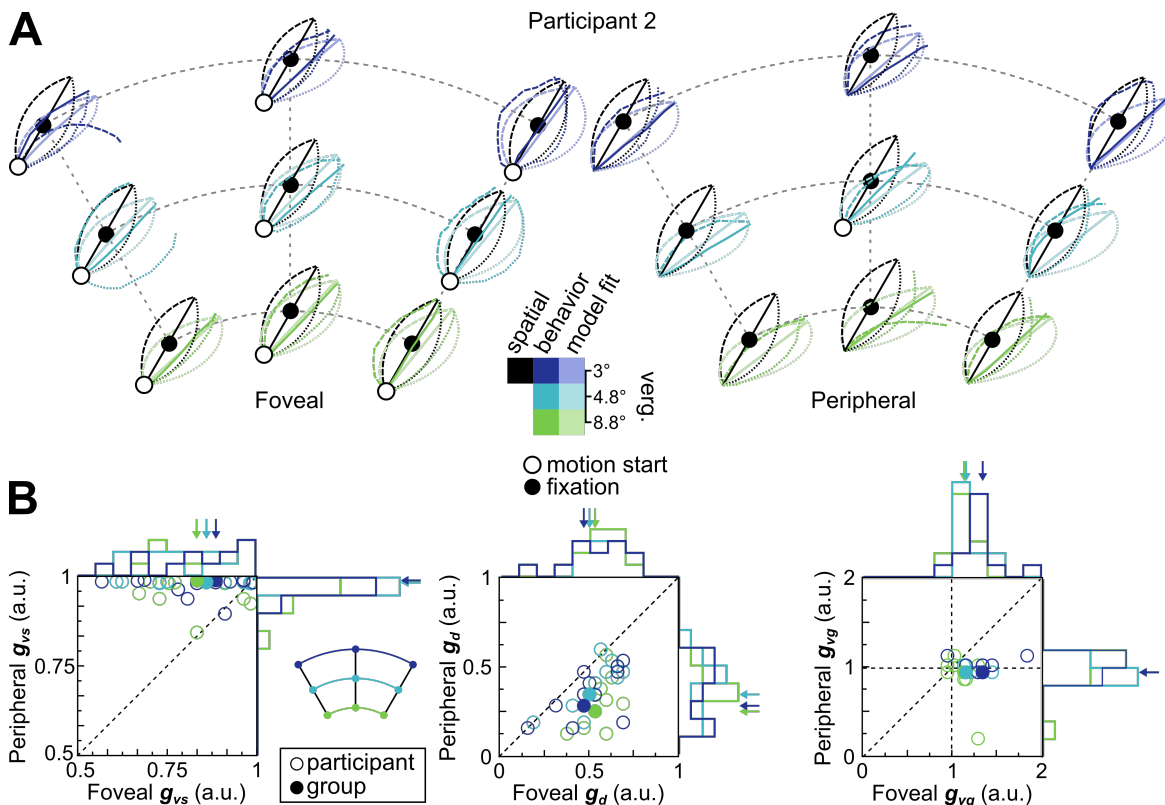


Figure 4: Results of model optimization. **A** Comparison of model outputs and spatial predictions with actual reconstructed trajectories after fitting version gain (g_{vs}), depth gain (g_d) and vergence gain (g_{vg}) parameters separately for each vergence distance and for foveal (left) and peripheral (right) motion conditions, for single participant (#2). **B** Group-level scatter plots showing peripheral versus foveal motion parameter fits for version gain (g_{vs} , left), depth gain (g_d , middle) and vergence gain (g_{vg}) (right). Open disks represent participant parameters and solid disks represent group-level parameters fit on all the data. Arrows above histograms represent group-level fit parameter locations along a given axis.

304

305 The parameters optimized for foveal and peripheral motion were distinct,
 306 suggesting that motion-in-depth perception varies with retinal eccentricity. For
 307 version gain, we found that participants accounted for 83% +/- 13% (mean +/-
 308 SD) of horizontal version during foveal motion, compared to 96% +/- 10% during
 309 peripheral motion (paired t-test: $t(35) = -5.22$, $p < 0.01$). Given that version
 310 compensation during foveal motion was incomplete, the apparent full
 311 compensation during peripheral motion could have been the result of the system

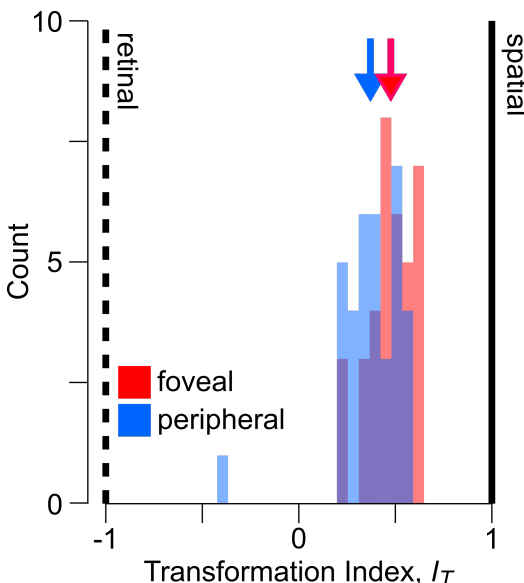
312 using the retinal location of the stimulus as a cue for current horizontal eye
313 orientation, effectively bypassing an explicit need for extraretinal signals. Next,
314 we found that the foveal depth gains accounted for 54% +/- 13% of depth speed
315 and was significantly greater than that for peripheral motion at 36% +/- 14%
316 (paired t-test: $t(35) = 8.70$, $p < 0.01$), indicating that motion in depth was
317 perceived to be faster when foveal. Finally, participants used a foveal vergence
318 gain of 1.22 +/- 0.18. In contrast, participants used a significantly smaller (and
319 more accurate) peripheral vergence gain of 0.98 +/- 0.15 (paired t-test: $t(35) =$
320 6.30, $p < 0.01$). These findings suggest that an underestimation of 3D eye
321 orientation signals during the transformation from retinal to spatial coordinates is
322 responsible for observed distortions to motion-in-depth perception.

323

324 Taken together, these three fit parameters allowed us to characterize the extent
325 to which the transformation from retinal to spatial coordinates occurred for each
326 participant. We computed a transformation index, I_T , represented by equation (1):

327
$$I_T = (D_R - D_S)/(D_R + D_S) \quad (1)$$

328 Where D_R and D_S are the Euclidian distances of each set of gain parameters from
329 the retinal and spatial hypotheses, respectively. For example, a purely spatial set
330 of gain parameters would be represented by $[g_{vs} \ g_{vg} \ g_d] = [1 \ 1 \ 1]$, corresponding
331 to a $D_S = 0$ and a $D_R = 1$; subsequently, $I_T = (1-0)/(1+0) = 1$. By the same logic, for
332 a purely retinal set of gains, $I_T = -1$. We present the distributions of these gain
333 parameters for each participant separated for foveal and peripheral motion,
334 merged across vergence fits, in Figure 5.



335

336 **Figure 5: Transformation indices (I_T) for foveal and peripheral motion.** Also
337 shown are the retinal (dashed) and spatial (solid) predictions, with means for
338 foveal (red) and peripheral (blue) motion represented by color-matched arrows.
339

340 I_T was significantly greater than 0 for both foveal (mean \pm SD: 0.48 ± 0.12 ;
341 $t(35) = 24.4$, $p < 0.01$) and peripheral motion (mean \pm SD: 0.37 ± 0.17 ; $t(35) =$
342 13.3 , $p < 0.01$), suggesting that, in both cases, reconstructed trajectories were
343 intermediate, but more spatial than retinal.

344

345 **Discussion**

346 We asked participants to estimate the motion-in-depth of an isolated disparity
347 stimulus and found large systematic errors that differed depending on viewing
348 eccentricity. We found that a simple model of the 3D eye-in-head geometry that
349 used inverse estimates of the ocular version angle, vergence angle and speed-
350 in-depth could capture the reconstructed trajectories well. For foveal motion, a
351 model that overestimated ocular vergence angle, underestimated ocular version
352 and target speed fit the perceived trajectories. For natural viewing, this result

353 suggests that additional monocular cues are necessary to accurately estimate
354 foveal motion in depth. Contrastingly, for peripheral motion, a model that
355 accurately estimated eye orientation signals fit the perceived reconstructions, but
356 this model also severely underestimated the speed in depth – more than during
357 foveal motion. In this condition, binocular eye orientations may have been
358 inferred using eccentricity-related monocular cues. Using a simple transformation
359 index computed from the inverse model fits, we found that spatial misperceptions
360 corresponded to a partial transformation of retinal motion into spatial coordinates,
361 regardless of retinal eccentricity.

362

363 We found that the visual system cannot use binocular retinal signals alone to
364 accurately estimate motion-in-depth at the fovea during fixation. This reliance on
365 monocular retinal cues and/or contextual depth cues is understandable given
366 their abundance in natural vision; however, absolute depth cannot be extracted
367 from monocular cues alone. Of course this is rarely an issue for typical viewing
368 when multiple relative depth cues are available. An additional reason why the
369 visual system might rely on often geometrically inaccurate cues potentially comes
370 from the idea that estimates of binocular eye orientation are unreliable (Blohm et
371 al., 2008; McGuire & Sabes, 2009), and these estimates might become even
372 more variable due to stochastic reference frame transformations (Alikhanian,
373 Carvalho, & Blohm, 2015). The head-to-world-centered coordinate transformation
374 required to extract depth from disparity could be stochastic (i.e., adding
375 uncertainty to the final depth estimate) and the fovea's high spatial acuity means

376 that monocular motion cues could be quite reliable for stereopsis (e.g., Ponce
377 and Born, 2008) This interpretation is consistent with various lines of evidence
378 showing a propensity of the visuomotor system to optimally account for
379 perceptual (Jessica K Burns & Nashed, 2011) and motor uncertainty (Jessica
380 Katherine Burns & Blohm, 2010; Schlicht & Schrater, 2007; Sober & Sabes,
381 2003) resulting from stochastic reference frame transformations (Alikhanian et
382 al., 2015), and is consistent with behavioral evidence from visuomotor updating
383 work (Fiehler, Rösler, & Henriques, 2010; Henriques, Klier, Smith, Lowy, &
384 Crawford, 1998; Medendorp, Goltz, Vilis, & Crawford, 2003; Murdison, Paré-
385 Bingley, & Blohm, 2013). Finally, the tendency of disparity-tuned neurons to
386 disproportionately prefer disparities <1 deg (DeAngelis & Uka, 2003) is another
387 clue that motion-in-depth at the fovea is represented differently in the visual
388 system than motion-in-depth in the periphery, where disparity magnitudes are
389 much larger (Blohm et al., 2008).

390

391 The peripheral motion case presents an apparently paradoxical finding: eye-in-
392 head orientation can be accurately estimated (likely using retinal eccentricity)
393 while target speed-in-depth is significantly underestimated relative to both its
394 spatial motion and its foveal motion. However, we provide *only* a disparity
395 stimulus to the observer regardless of retinal location, and the relative
396 contribution of disparity to depth perception decreases with eccentricity (Held et
397 al., 2012). The observed percept of compressed motion in the periphery is
398 therefore in line with the idea of a lower-weighted contribution of disparity cues

399 (Held et al., 2012), while changes in defocus blur of the point stimulus were likely
400 negligible. In agreement with this idea, some early psychophysical findings reveal
401 that such a lateral compression could be due to greater relative uncertainty in the
402 estimate of the depth motion component for motion in the periphery (Rokers et
403 al., 2017, pre-print). Determining whether motion-in-depth perception is based on
404 such a statistically optimal combination of disparity, retinal defocus blur and
405 extraretinal cues therefore represents a potential extension of this work.

406

407 To isolate for horizontal disparity as the primary cue for depth perception, we
408 removed any contribution of visuomotor feedback by restricting movements of
409 the eyes and head. We determined the role of *static* eye orientation signals in
410 interpreting a *dynamic, moving* stimulus, although in natural viewing our eyes
411 and head are often moving as well. Both disparity and eye movements contribute
412 to depth perception but the precise nature of these contributions, and how they
413 might depend on one another, is unclear. For example, vergence angle
414 corresponds to perceived depth during the kinetic depth effect (Ringach,
415 Hawken, & Shapley, 1996), but artificially inducing disparity changes between
416 correlated (and anti-correlated) random-dot stimuli can cause the eyes to rapidly
417 converge (or diverge) without any perception of depth (Masson, Bussetti, &
418 Miles, 1997). On the neural level, disparity is coded in V1 without a necessary
419 perception of depth (Cumming & Parker, 1997). Psychophysics work has shown
420 that vergence eye movements are beneficial for judging the relative depth of
421 stimuli (Foley & Richards, 1972), but to our knowledge no one has investigated

422 the extent to which these signals are used to solve the geometry for absolute
423 depth.

424

425 In addition, by restricting the orientations of the eyes and head we removed
426 feedback due to motion parallax and changes in vertical disparity. Importantly,
427 providing such dynamic feedback has been shown to improve motion-in-depth
428 perception in virtual reality (Fulvio & Rokers, 2017). Although vertical disparity
429 naturally varies during normal ocular orienting, we designed our task to keep
430 vertical disparity constant for a given gaze location. This manipulation not only
431 removed vertical disparities due to changes in cyclovergence, but also vertical
432 disparities due to changes in head orientation (Blohm et al., 2008). These natural
433 changes in vertical disparity during eye and head movements likely serve as
434 another informative dynamic cue for judging motion-in-depth under normal
435 viewing contexts. For the above reasons, presenting participants with a dynamic,
436 motion-tracked version of our task could therefore represent an important
437 extension of this work.

438

439 From an evolutionary perspective, it is unclear why the visual system would
440 underestimate binocular cues when estimating motion in depth with static gaze.
441 Indeed, in an enriched visual environment there are often sufficient monocular
442 cues available to the visual system to be able to judge relative depth. During
443 everyday viewing in natural contexts, this is often the case; especially for self-
444 generated motion in depth. On the other hand, our findings suggest that in some

445 special cases without an enriched viewing context such a monocular strategy
446 fails. To illustrate this point, consider two edge cases: juggling and firefly-
447 catching. Expert jugglers learn to fixate the apex of the balls' trajectory,
448 presumably taking advantage of a learned internal model of the balls' ballistic
449 trajectory (resulting from manual motor commands) combined with various
450 monocular motion cues to intercept each ball. Alternatively, consider the case of
451 attempting to catch a firefly in darkness: fixating while attempting this is intuitively
452 a bad idea because the flight of a firefly is largely unpredictable. Instead, to catch
453 the fly, a better strategy might be to visually track its motion. Such a strategy
454 would allow for the use of consistent visuomotor feedback, allowing the
455 construction of a predictive model of the fly's path. Thus, follow-up experiments
456 investigating the interplay between (1) availability of monocular cues, (2)
457 predictability of object physics and (3) facilitation from visuomotor learning would
458 be informative of how our brain constructs motion-in-depth percepts.

459

460 **Conclusions**

461 We quantified the extent to which visual perception accounts for the 3D geometry
462 of the eyes and head when interpreting motion in depth under static viewing
463 conditions. We found that participants underestimated 3D binocular eye
464 orientations, leading to different spatial motion percepts for identical egocentric
465 trajectories. To perceive and successfully navigate through the 3D world, our
466 findings suggest that perception must supplement binocular disparity signals with
467 binocular eye and head orientation estimates, monocular depth cues and

468 dynamic visuomotor feedback. It remains to be seen, however, what the precise
469 contributions and relative weightings of each of these cues might be.

470

471 **Acknowledgments**

472

473 The authors want to thank [REDACTED]. This work was supported by NSERC
474 (Canada), CFI (Canada), the Botterell Fund (Queen's University, Kingston, ON,
475 Canada) and ORF (Canada). TSM was also supported by DAAD (Germany) and
476 DFG (Germany).

477

478 **References**

479 Alikhanian, H., Carvalho, S. R., & Blohm, G. (2015). Quantifying effects of
480 stochasticity in reference frame transformations on posterior distributions.
481 *Frontiers in Computational Neuroscience*, 9(July), 1–9.
482 <http://doi.org/10.3389/fncom.2015.00082>

483 Backus, B. T., Banks, M. S., Van Ee, R., & Crowell, J. A. (1999). Horizontal and
484 vertical disparity, eye position, and stereoscopic slant perception. *Vision
485 Research*, 39(6), 1143–1170. [http://doi.org/10.1016/S0042-6989\(98\)00139-4](http://doi.org/10.1016/S0042-6989(98)00139-4)

486 Banks, M. S., & Backus, B. T. (1998). Extra-retinal and perspective cues cause
487 the small range of the induced effect. *Vision Research*, 38(2), 187–194.
488 [http://doi.org/10.1016/S0042-6989\(97\)00179-X](http://doi.org/10.1016/S0042-6989(97)00179-X)

489 Batista, A. P., Buneo, C. A., Snyder, L. H., & Andersen, R. A. (1999). Reach
490 plans in eye-centered coordinates. *Science*, 285(5425), 257–60.

491 Blohm, G., & Crawford, J. D. (2007). Computations for geometrically accurate
492 visually guided reaching in 3-D space. *Journal of Vision*, 7(5), 1–22.
493 <http://doi.org/10.1167/7.5.4.Introduction>

494 Blohm, G., Khan, A. Z., Ren, L., Schreiber, K. M., & Crawford, J. D. (2008).
495 Depth estimation from retinal disparity requires eye and head orientation
496 signals. *Journal of Vision*, 8(16), 1–23. <http://doi.org/10.1167/8.16.3.doi>

497 Burns, J. K., & Blohm, G. (2010). Multi-sensory weights depend on contextual
498 noise in reference frame transformations. *Frontiers in Human Neuroscience*,
499 4(December), 1–15. <http://doi.org/10.3389/fnhum.2010.00221>

500 Burns, J. K., & Nashed, J. Y. (2011). Head roll influences perceived hand

501 position. *Journal of Vision*, 11, 1–9. <http://doi.org/10.1167/11.9.3>.

502 Chang, S. W. C., Papadimitriou, C., & Snyder, L. H. (2009). Using a compound
503 gain field to compute a reach plan. *Neuron*, 64(5), 744–55.
504 <http://doi.org/10.1016/j.neuron.2009.11.005>

505 Cumming, B. G., & Parker, a J. (1997). Responses of primary visual cortical
506 neurons to binocular disparity without depth perception. *Nature*, 389(6648),
507 280–3. <http://doi.org/10.1038/38487>

508 DeAngelis, G. C., & Uka, T. (2003). Coding of horizontal disparity and velocity by
509 MT neurons in the alert macaque. *Journal of Neurophysiology*, 89(2), 1094–
510 111. <http://doi.org/10.1152/jn.00717.2002>

511 Fiehler, K., Rösler, F., & Henriques, D. Y. P. (2010). Interaction between gaze
512 and visual and proprioceptive position judgements. *Experimental Brain
513 Research*, 203(3), 485–98. <http://doi.org/10.1007/s00221-010-2251-1>

514 Foley, J. M., & Richards, W. (1972). Effects of voluntary eye movement and
515 convergence on the binocular appreciation of depth. *Perception &
516 Psychophysics*, 11(6), 423–427. <http://doi.org/10.3758/BF03206284>

517 Fulvio, J. M., & Rokers, B. (2017). Use of cues in virtual reality depends on visual
518 feedback. *Scientific Reports*, 7(1), 16009. [http://doi.org/10.1038/s41598-017-16161-3](http://doi.org/10.1038/s41598-017-
519 16161-3)

520 Guan, P., & Banks, M. S. (2016). Stereoscopic depth constancy. *Philosophical
521 Transactions of the Royal Society B: Biological Sciences*, 371(20150253),
522 1–15. <http://doi.org/10.1098/rstb.2015.0253>

523 Held, R. T., Cooper, E. A., & Banks, M. S. (2012). Blur and Disparity Are

524 Complementary Cues to Depth. *Current Biology*, 22(5), 426–431.

525 <http://doi.org/10.1016/j.cub.2012.01.033>

526 Henriques, D. Y. P., Klier, E. M., Smith, M. A., Lowy, D., & Crawford, J. D.

527 (1998). Gaze-centered remapping of remembered visual space in an open-

528 loop pointing task. *The Journal of Neuroscience*, 18(4), 1583–1594.

529 Masson, G. S., Busettini, C., & Miles, F. A. (1997). Vergence eye movements in

530 response to binocular disparity without the perception of depth. *Nature*, 389,

531 283–286.

532 McGuire, L. M. M., & Sabes, P. N. (2009). Sensory transformations and the use

533 of multiple reference frames for reach planning. *Nature Neuroscience*, 12(8),

534 1056–1061. <http://doi.org/10.1038/nn.2357>. Sensory

535 Medendorp, W. P., Goltz, H. C., Vilis, T., & Crawford, J. D. (2003). Eye-centered

536 remapping of remembered visual space in human parietal cortex. *Journal of*

537 *Vision*, 3(9), 125a. <http://doi.org/10.1167/3.9.125>

538 Mon-Williams, M., & Tresilian, J. R. (1999). Some recent studies on the

539 extraretinal contribution to distance perception. *Perception*, 28(2), 167–181.

540 <http://doi.org/10.1068/p2737>

541 Mon-Williams, M., & Tresilian, J. R. (2000). Ordinal depth information from

542 accommodation? *Ergonomics*, 43(3), 391–404.

543 <http://doi.org/10.1080/001401300184486>

544 Mon-Williams, M., Tresilian, J. R., & Roberts, A. (2000). Vergence provides

545 veridical depth perception from horizontal retinal image disparities.

546 *Experimental Brain Research*, 133(3), 407–413.

547 <http://doi.org/10.1007/s002210000410>

548 Murdison, T. S., Paré-Bingley, C. A., & Blohm, G. (2013). Evidence for a retinal
549 velocity memory underlying the direction of anticipatory smooth pursuit eye
550 movements. *Journal of Neurophysiology*, 110, 732–747.

551 <http://doi.org/10.1152/jn.00991.2012>

552 Ponce, C. R., & Born, R. T. (2008). Stereopsis. *Current Biology : CB*, 18(18),
553 R845–R850. <http://doi.org/10.1016/j.cub.2008.07.006>

554 Ringach, D. L., Hawken, M. J., & Shapley, R. (1996). Binocular eye movements
555 caused by the perception of three-dimensional structure from motion. *Vision*
556 *Research*, 36(10), 1479–1492. [http://doi.org/10.1016/0042-6989\(95\)00285-5](http://doi.org/10.1016/0042-6989(95)00285-5)

557 Rokers, B., Fulvio, J. M., Pillow, J., & Cooper, E. A. (2017). Systematic
558 misperceptions of 3D motion explained by Bayesian inference, *bioRxiv (pre-*
559 *print*), 1–46. <http://doi.org/10.1101/149104>

560 Schlicht, E. J., & Schrater, P. R. (2007). Impact of Coordinate Transformation
561 Uncertainty on Human Sensorimotor Control. *Journal of Neurophysiology*,
562 97, 4203–4214. <http://doi.org/10.1152/jn.00160.2007>.

563 Sober, S. J., & Sabes, P. N. (2003). Multisensory integration during motor
564 planning. *Journal of Neuroscience*, 23(18), 6982–92.

565 Zannoli, M., Love, G. D., Narain, R., & Banks, M. S. (2016). Blur and the
566 perception of depth at occlusions. *Journal of Vision*, 16(6), 1–25.

567 <http://doi.org/10.1167/16.6.17.doi>

568 Zannoli, M., & Mamassian, P. (2011). The role of transparency in da Vinci
569 stereopsis. *Vision Research*, 51(20), 2186–2197.

570 <http://doi.org/10.1016/j.visres.2011.08.014>

571